Università degli Studi di Napoli
"Federico II"

Dottorato in Scienze Biomorfologiche e Chirurgiche

XXXIII Ciclo

Direttore Prof. A. Cuocolo

Aetiology and prognostic significance of non-infarct pattern late gadolinium enhancement in patients with coronary artery disease: a cardiovascular magnetic resonance prospective outcome study

Tutor:

Ch.mo Dott.
Massimo Imbriaco

Candidato:

Dott.ssa
Francesca Musella

Index

Aetiology and prognostic significance of non-infarct pattern late gadolinium enhancement in patients with coronary artery disease: a cardiovascular magnetic resonance prospective outcomes study

Introduction

Current tools to identify patients at high risk of sudden cardiac death (SCD) are limited. Specifically, left ventricular ejection fraction (LVEF) is an imprecise metric and innovative approaches are required to identify arrhythmogenic substrate beyond this measure. SCD risk prediction is of notable importance for patients with coronary artery disease (CAD) as these individuals are already in an intermediate risk group.[1] It is therefore appropriate to evaluate the utility of novel prediction tools to identify high-risk patients within this cohort.

In patients with chronic CAD, re-entrant ventricular tachycardia (VT) is the presumed mechanism underpinning the majority of SCD cases. Septa of replacement extracellular fibrosis (resultant from necrosing myocytes) perforating bundles of surviving myocytes can provide an arrhythmogenic milieu capable of facilitating the re-entry circuit.[2] These areas of heterogenous tissue, more recently termed the 'peri-infarct' or 'gray' zone, are typically located at the transition point between viable myocardium and compact scar and are hypothesised to contain the substrate for slow conduction and fixed/functional block that initiate and maintain VT.[3] Implantable cardioverter defibrillators (ICD) can treat re-entrant arrhythmia and have been shown to protect against a high proportion of SCD.[4] Decisions regarding primary prevention ICD implantation centre around evaluation of NYHA class alongside dichotomous assessment of LV systolic function using a LVEF cut-off of 30-35%. Typically

assessed at a solitary timepoint, this fails to take into account the dynamic nature of the variable.[5,6]

Late Gadolinium Enhancement on Cardiac Magnetic Resonance (LGE-CMR) non-invasively identifies myocardial fibrosis with high spatial resolution and has good histological correlation in CAD models.[7] Additionally, quantification of core infarct and the adjacent peri-infarct zone (PIZ) has been shown to associate with ventricular arrhythmia and all-cause mortality in CAD cohorts.[8,9] More recently, LGE-CMR has been used to evaluate complex scar geometry, predominantly in tandem with electroanatomical voltage mapping (EAVM) or computational modelling techniques.[3,10,11] Despite recent advances however, important questions remain on the utility of advanced scar characterisation by CMR to predict SCD, particularly in prospectively recruited cohorts. We performed LGE quantification, in combination with bespoke computational analysis of shape-based scar features, to provide novel mechanistic insight into the drivers of SCD in prospectively investigated patients with CAD.

Methods

Study design

Patients referred for evaluation of ischaemic heart disease with LGE-CMR were prospectively recruited into a registry between August 2009 and January 2016. The registry complied with the Declaration of Helsinki and the Southampton & South West Hampshire Research Ethics Committee approved the protocol. All patients provided informed written consent. CMR was undertaken on a 1.5 Tesla scanner (Sonata/Avanto, Siemens). Steady-state free precession sequences were performed to produce long and short-axis cine images. Gadolinium-based contrast agent was injected intravenously and an inversion recovery gradient echo sequence was undertaken to acquire the LGE datasets at ~10mins, typically in two phase encoding directions. The LGE images were obtained in the long axis planes and then in continuous short slices to cover the entire left ventricle (LV). The LGE image slice thickness was 8mm with a 2mm gap, resulting in an in-plane resolution of ~2.2mm x ~1.6mm.

The inclusion criteria for the study were severe epicardial CAD, prior coronary revascularisation or documented history of prior myocardial infarction (confirmed on CMR). Severe epicardial CAD was defined as ≥75% stenosis in the left main stem/proximal left anterior descending artery or ≥75% in 2 epicardial coronary arteries. Exclusion criteria included Class I indication for a secondary prevention ICD, myocardial infarction (MI) within 40 days prior to CMR, severe primary valvular disease, previous valvular intervention or high suspicion of concomitant hypertrophic or infiltrative cardiomyopathy.

Cardiovascular Magnetic Resonance analysis

Biventricular volumes and LV mass were determined using CMRtools (Cardiovascular Imaging Solutions, London, United Kingdom). LGE quantification (including PIZ analysis) was performed by a Level 3 accredited CMR operator blinded to the clinical outcomes. Infarct analysis was undertaken using the full width at half maximum (FWHM) method on specialised software (CVI42, Circle Cardiovascular Imaging Inc, Calgary, Canada). Epicardial and endocardial contours were drawn from the short-axis LGE slices and a region of interest was created within an area of core infarct. The PIZ was then defined as signal intensity (SI) between 35%-49% of the core infarct.

Evaluation of scar microstructure

We aimed to identify key relationships and microstructure features within the myocardial fibrosis to gain mechanistic insight into the drivers of life-threatening ventricular arrhythmia. Linked anonymised LGE slices were optimised for computational analysis. Harnessing both the raw LGE images and corresponding FWHM slice masks, we extracted data relating to 7 groups of morphological and texture related scar features (Table 1).[10,12] The scar features were computed for each individual slice and then aggregated across the short-axis stack to better represent LGE topology throughout the LV where applicable.

Clinical endpoints and follow up data collection

Patients were followed up using health questionnaires alongside primary and secondary care documentation. ICD reports, death certificates and post-mortem results

were requested as necessary. Survival status was confirmed via the UK NHS Digital service to ensure that no deaths were omitted. The duration of follow-up was determined from the date of CMR prior to consent until an endpoint was confirmed or until the most recent patient contact date. Event times were calculated from the date of the preceding CMR up until a maximum of 10 years. All clinical outcomes were adjudicated by an independent panel of experienced cardiologists blinded to the LGE data. The *a priori* primary endpoint was a composite of sudden cardiac death or aborted sudden cardiac death. Sudden cardiac death was defined as a death that occurred unexpectedly, including scenarios where symptom duration was ≤1hr, following an identified arrhythmia/unsuccessful resuscitation or in circumstances where the patient was witnessed alive ≤24hr prior to death and without another identifiable cause of death.[13] Aborted SCD was defined as appropriate ICD shock for a ventricular tachyarrhythmia, effective resuscitation following ventricular fibrillation or haemodynamically unstable VT requiring electrical cardioversion.[14] The prespecified secondary endpoints included: i) major heart failure (HF) composite of HF hospitalisation (admission to hospital of ≥24hr/encompassing 1 calendar day requiring initiation or escalation of HF therapies), HF death (in the context of progressive clinical features of HF), or cardiac transplantation/left ventricular assist device insertion, ii) all-cause mortality and iii) SCD or aborted SCD in patients with a LVEF ≥35%.

Statistical analysis

Baseline characteristics were summarised in the total cohort as frequency (%) for categorical variables and mean (standard deviation, σ) or median (interquartile range, IQR) where appropriate for continuous variables. Characteristics were compared between patients with a PIZ mass <median versus those with a PIZ mass ≥median using 2-sample t-tests or Mann-Whitney U tests for continuous variables and χ^2 test or Fisher's exact tests for categorical variables.

Kaplan-Meier curves were plotted to describe the cumulative incidence of the primary outcome by tertiles of PIZ mass and core infarct mass over follow-up, compared using the logrank test. Univariable and multivariable analyses of the primary and secondary outcomes were performed using Cox regression modelling. To investigate the utility of LGE quantification in the prediction of the primary outcome, two multivariable models were generated. First, to mirror current clinical guidelines for ICD implantation, a model using binary cut-offs of LVEF <35% and NYHA class >1 was generated (Model 1). Second, a model was fitted using baseline covariates associated with the primary outcome (Model 2). To select this model, a forward stepwise procedure was applied with $p<0.10$ as the criterion for inclusion, forcing in known predictors of the outcome from existing literature (age, sex and LVEF). In both Models 1 and 2, core infarct mass and PIZ mass were then simultaneously added to assert whether either metric was independently associated with the primary outcome. Model performance was assessed using the Harrel's C-statistic. Additionally, competing risk analysis was performed using Fine-Gray subdistribution hazard modelling. The non-arrhythmic secondary endpoints were assessed using the

multivariable approach described in Model 2 and subgroup analysis of patients with LVEF ≥35% were adjusted for age, sex and LVEF. A P-value of ≤0.05 was taken as significant. Statistical analysis was performed on Stata version 17 (StatCorp) and Python v3.7.4.

Results

734 patients were assessed for eligibility with the final cohort consisting of 437 patients. The mean age was 64 (σ 9.9 years), mean LVEF 47% (σ 16.8%) and 95% of patients had severe CAD or had previously undergone coronary revascularisation. All 25 (5%) patients without evidence of severe CAD had a history of prior myocardial infarction, confirmed on CMR. Baseline characteristics are described in Table 2. The median PIZ mass was 8.8g (IQR: 4.2g-14.4g) and core mass was 17.6g (IQR: 6.5g-30.2g). Patients with a PIZ mass above the median were more likely to be men (P=0.004), current smokers (P=0.01), have significant CAD (P<0.001), have a history of prior MI (P<0.001) and be prescribed diuretic therapy or medications acting on the renin-angiotensin aldosterone system (P<0.001).

Primary endpoint

Utility of core infarct mass and PIZ mass to predict the composite of SCD or SCD.

At 10 years follow up, 49 patients (11.2%) had experienced the primary outcome (29 patients experiencing aborted SCD and 20 patients experiencing SCD). Autopsy data was available for 12 of the deaths assigned as SCD. Cumulative incidence of the primary outcome by tertiles of PIZ mass suggest that patients in higher tertiles had an increased risk of the primary outcome (10-year risk 0.7%, 24.0% and 37.8% for patients with PIZ mass <5.66g, 5.66-12.28g and ≥12.29g respectively, P<0.001, Fig.1). Similarly, patients in the higher tertiles of core mass had an increased risk of the primary outcome (10-year risk 3.7%, 24.0% and 34.6% for patients with core mass <9.39, 9.39-25.21g and ≥25.22g respectively, P<0.001, Fig.1). On univariable analysis, an increase in PIZ mass and core infarct mass was significantly

associated with an increased risk of the primary outcome (per gram: HR 1.12, 95% CI 1.09-1.15, P<0.001 and HR 1.05, 95% CI 1.04-1.06, P<0.001 respectively).

After adjustment for the variables in Model 1 (LVEF <35% and NYHA Class II,III or IV), both PIZ mass and core infarct mass remained independently associated with the primary outcome (per gram: HR 1.07, 95% CI 1.02-1.12, P=0.002 and HR 1.03, 95% CI 1.01-1.05, P=0.01 respectively, Fig.2) and improved the ability of the model to predict the primary endpoint of SCD or aborted SCD (C-statistic from 0.64 to 0.79). Severely impaired LVEF was not associated with the primary endpoint on multivariable analysis (HR 1.65, 95% CI 0.90-3.03, P=0.11, Fig.2). Additionally, PIZ mass and core infarct mass remained independently associated with the primary endpoint after adjusting for non-sudden death on competing risk analysis (per gram: subdistribution HR 1.07, 95% CI 1.03-1.12, P=0.001 and subdistribution HR 1.03, 95% CI 1.01-1.04, P=0.003 respectively, Fig.3).

Using Model 2, PIZ mass and core infarct remained independently associated with the primary outcome after adjusting for baseline covariates (per gram: HR 1.07, 95% CI 1.02-1.12, P=0.005 and HR 1.02, 95% CI 1.00-1.05, P=0.03 respectively, Fig.4) and improved the discrimination of the model to predict the primary endpoint (C-statistic 0.76 to 0.82). Again, LVEF was not associated with the primary endpoint on multivariable analysis (per %: HR 0.99, 95% CI 0.0.97-1.02, P=0.63, Fig.4).

Utility of scar microstructure analysis to predict the composite of SCD or SCD

In examining the PIZ and core infarct microstructure, we identified 28 individual features that remained significantly associated with the primary endpoint on multivariable analysis (Table 3). These were catalogued according to the central

microstructure component with the 6 groups containing features that remained significantly associated with the primary endpoint on multivariable analysis, Fig. 5.

The best performing model in each group included the following features; PIZ gradient, number of PIZ components, core infarct radiality, core infarct interface area, core infarct entropy and variation in core infarct transmurality (Fig.6). No individual scar feature remained significantly associated with the primary endpoint when absolute core infarct mass and PIZ mass were added to the multivariable model.

Secondary endpoints

Major heart failure event

During follow-up, 78 (17.9%) patients experienced a major heart failure event. On univariable analysis, both PIZ and core infarct mass were significantly associated with the outcome (per gram: HR 1.06, 95% CI 1.03-1.08, P<0.001 and HR 1.02, 95% CI 1.01-1.04, P<0.001 respectively). On multivariable analysis however, there was no significant association between either scar metric and this secondary endpoint (PIZ mass per gram: HR 1.02, 95% CI 0.98-1.06, P=0.35 and core infarct mass per gram HR 1.00, 95% CI 0.98-1.02, P=0.77, Figure).

All-cause mortality

There were 138 (31.6%) deaths during the follow-up period (92 cardiovascular deaths, 46 non-cardiovascular deaths). On univariable analysis, PIZ and core infarct mass were significantly associated with the endpoint (per gram: HR 1.05, 95% CI 1.03-1.07, P<0.001 and HR 1.02, 95% CI 1.01-1.03, P<0.001 respectively). On multivariable analysis, PIZ mass remained independently associated with mortality

(per gram: HR 1.04, 95% CI 1.01-1.08, P=0.02, Fig.8) and marginally improved the discrimination ability of the model to predict the outcome (C-statistic 0.74 to 0.75). Core infarct mass was not significantly associated with the endpoint when both scar metrics were included in the model (per gram: HR 1.00, 95% CI 0.98-1.02, P=0.96, Fig.8).

Composite of sudden cardiac death or aborted sudden cardiac death in patient with LVEF ≥35%.

25 out of 319 patients with LVEF ≥35% experienced a SCD or aborted SCD. On univariable analysis, both PIZ mass and core infarct mass were associated with the endpoint (per gram: HR 1.09, 95% CI 1.04-1.14, P<0.001 and HR 1.04, 95% CI 1.02-1.06, P<0.001 respectively). Neither PIZ mass or core infarct mass remained significantly associated with the primary endpoint when both scar metrics were included in the model (per gram: HR 1.03, 95% CI 0.94-1.11, P=0.56 and HR 1.03, 95% CI 0.99-1.07, P=0.11 respectively, Fig.9). Computational analysis of the LGE images in patients with LVEF ≥35% highlighted 4 specific scar features that were significantly associated with the primary endpoint on multivariable analysis (adjusted for age, sex and LVEF); standard deviation of core infarct transmurality, PIZ entropy, core infarct entropy and the combined entropy from both the PIZ and core infarct.

Discussion

To our knowledge, this is the first prospective study assessing the utility of multiscale myocardial fibrosis characterization by CMR to predict SCD in prospectively investigated patients with CAD. The principal findings are: i) PIZ mass and core infarct mass independently predict SCD after adjusting for clinical parameters used in ICD implantation decisions; ii) Reduced LVEF does not predict SCD when LGE parameters are included in the multivariable models; iii) Neither scar metric associates with major heart failure events on multivariable analysis; iv) Bespoke computational analysis identified a group of clinically plausible scar microstructure features that associate with SCD.

LGE-CMR predictors of SCD in stable CAD

Multiple observational studies in CAD cohorts have demonstrated the role of PIZ quantification by LGE-CMR to identify patients at increased risk of all-cause mortality[15], inducibility of VT during electrophysiology study[16] and appropriate ICD therapy.[17] The majority of these studies either restricted recruitment to patients with impaired LVEF or those with prior ICD insertion. Additionally, these studies typically included individuals with an existing secondary prevention ICD indication and thus novel CMR metrics were unlikely to alter management decisions. Zegard et al recently published a large study assessing the association between LGE and SCD in a cohort of CAD patients with a broad range of LVEF.[18] Although retrospective, their results were notably similar to our findings and demonstrate the value of myocardial fibrosis quantification to predict SCD in patients with CAD. As with their study, we also demonstrate that PIZ mass has a stronger association with the primary endpoint

as compared to core infarct mass. This growing body of work continues to support the hypothesis that the PIZ contains myocardial substrate capable of initiating and maintaining lethal ventricular arrhythmia. In our study, reduction in LVEF did not predict the primary endpoint following addition of the scar metrics to either multivariable model. This is clinically relevant as LVEF calculation remains the central measure used in ICD implantation decisions, driven by inclusion criteria of the seminal trials assessing the utility of primary prevention ICD therapy.[19,20] It is well appreciated however that impaired LVEF does not directly identify arrhythmogenic myocardial substrate. Up to 70% of SCD cases in CAD populations occur in subjects without severely reduced LVEF[21] and there remains a paucity of evidence identifying a convincing causal relationship between LVEF and SCD.[22] Conversely, myocardial fibrosis is a mechanistically plausible metric in SCD prediction and may also represent a relatively static parameter in patients who do not suffer a subsequent MI. Neither scar metric predicted major heart failure events on multivariable analysis. Additionally, competing risk analysis demonstrated the association between both scar metrics and the primary endpoint after adjusting for non-sudden death. These results highlight the potential utility of LGE quantification as a precision tool in event prediction; hypothetically targeting ICD implantation to CAD patients with high future arrhythmic risk and lower future non-arrhythmic event risk. Individuals without severely reduced LVEF represent the largest cohort of SCD patients and yet are not captured in primary prevention ICD guidelines. We showed that in patients with preserved LV systolic function, LGE quantification predicted SCD on univariable analysis. The lack of the statistical significance when both PIZ mass and core infarct

mass were added to the multivariable model likely pertains to being underpowered for this subgroup analysis.

Computational analysis of the LGE images

The computational analysis of the LGE images permitted mechanistic interrogation into the key morphological and texture-based scar features driving the primary outcome, providing an additional layer of granularity above the raw quantification data. The majority of these features already have a considerable evidence base detailing their association with ventricular arrhythmia, predominantly from studies harnessing EAVM in combination with CMR. First, a key feature that associated with the primary endpoint was LGE interface area. This metric describes the extent of the border between LGE and adjacent tissue, typically the PIZ. This parameter has been found to associate with major arrhythmic events in dilated cardiomyopathy with simulation modelling describing a plausible mechanism of action to promote unidirectional conduction block.[10] Furthermore, in a mixed cohort of ischaemic and non-ischaemic heart disease, scar borderzone has been found to harbor critical VT isthmus sites.[23] Second, multiple aggregates pertaining to core scar transmurality and radiality were associated with the primary endpoint on multivariable analysis. Core scar transmurality on CMR has been associated with reduction in electrogram voltages on EAVM.[24] Furthermore, critical VT isthmus sites have been found in close proximity to areas of increasingly transmural scar.[23] LGE radiality has previously been investigated in non-ischaemic cohorts but was not significantly associated with major arrhythmic events.[10] Third, recent studies have assessed the utility of scar entropy to predict life threatening arrhythmia. Scar entropy describes the

level of disorder or heterogeneity within a region of myocardial fibrosis[25]. Androulaskis et al demonstrated an association between high myocardial fibrosis entropy and ventricular arrhythmia in patients post myocardial infarction.[26] Forth, the PIZ gradient represents another texture related feature that associated with our primary endpoint. This feature details the rate in change of SI within a region of interest and a high LGE gradient, representing an extreme change in SI, has previously been shown to associate with patients deemed at high risk of life-threatening arrhythmia.[27] Finally, a high number of PIZ components per LGE slice was associated with our primary endpoint. A correlate of this feature, PIZ channels, has recently been shown to associate with appropriate ICD therapy.[28] Additionally, the number of LGE components was found to be associated with functional block and reentry on paced simulation models in patients with dilated cardiomyopathy.[12] In summary, there is growing body of evidence describing the association between complex scar analysis on CMR and either ventricular arrhythmia or crucial VT sites on EAVM. We have described for the first time the association between numerous complex shape-based scar features and SCD in prospectively investigated patients with stable CAD.

Limitations

This study is a single center study in patients referred to a tertiary cardiovascular hospital. As such, the generalizability of the results may be questioned and the potential for referral bias is introduced. Our results are similar however to previous studies[15,18] and our patient cohort were referred from a broad base of secondary and tertiary hospitals. We do appreciate that our study contains a high percentage of male and caucasian patients and thus the results may not be applicable to female patients and non-caucasian populations. Concerns regarding the ability of 2-dimensional LGE to accurately characterise the PIZ have been raised. This principally surrounds the issue of partial voluming where imaged voxels contain both cleanly demarcated core scar and adjacent normal myocardium. This results in an intermediate signal due to the limited spatial resolution and not because of a region of viable myocytes interspersed with collagen. Future studies harnessing 3-dimensional LGE would allow for whole-heart coverage with reduced voxel dimensions and improved spatial resolution. The elimination of slice gaps would permit more detailed characterization of the relationship of LGE features along the slice direction (e.g. increasing the confidence to describe potential VT conduction channels). We appreciate that we only performed LGE quantification by the FWHM method and recent studies have highlighted increased association with SCD using standard deviation approaches.[18] FWHM has however been found to be the most reproducible technique[29] and the majority of studies assessing PIZ quantification and long-term clinical outcomes have harnessed this methodology.[15]

Conclusions

SCD is a prevalent and tragic event afflicting patient with CAD and current risk stratification approaches remain insensitive and nonspecific.[30] Our study provides novel prospective data demonstrating the value of myocardial fibrosis characterization by CMR to predict SCD in a cohort of stable CAD patients. We also highlight the limitation of LVEF calculation in SCD risk prediction. Multicenter trials should now be considered utilizing appropriate cut-offs for these LGE metrics above which patients are randomized to ICD implantation or conventional medical therapy. Such trials would be most impactful in cohorts not captured by current ICD guidelines, notably patients with mild to moderate LV systolic impairment.

References

1. Fishman GI, Chugh SS, DiMarco JP, Albert CM, Anderson ME, Bonow RO, Buxton AE, Chen P-S, Estes M, Jouven X, Kwong R, Lathrop DA, Mascette AM, Nerbonne JM, O'Rourke B, Page RL, Roden DM, Rosenbaum DS, Sotoodehnia N, Trayanova NA, Zheng Z-J. Sudden Cardiac Death Prediction and Prevention. *Circulation* 2010;**122**:2335–2348.

2. Bakker JM de, Capelle FJ van, Janse MJ, Tasseron S, Vermeulen JT, Jonge N de, Lahpor JR. Slow conduction in the infarcted human heart. "Zigzag" course of activation. *Circulation* 1993;**88**:915–926.

3. Sramko M, Hoogendoorn JC, Glashan CA, Zeppenfeld K. Advancement in cardiac imaging for treatment of ventricular arrhythmias in structural heart disease. *EP Europace* 2019;**21**:383–403.

4. Greenberg H, Case RB, Moss AJ, Brown MW, Carroll ER, Andrews ML. Analysis of mortality events in the multicenter automatic defibrillator implantation trial (MADIT-II). *Journal of the American College of Cardiology* Elsevier Masson SAS; 2004;**43**:1459–1465.

5. Myerburg RJ, Goldberger JJ. Sudden Cardiac Arrest Risk Assessment. *JAMA Cardiology* 2017;**2**:689.

6. Goldberger JJ, Buxton AE, Cain M, Costantini O, Exner D v., Knight BP, Lloyd-Jones D, Kadish AH, Lee B, Moss A, Myerburg R, Olgin J, Passman R, Rosenbaum D, Stevenson W, Zareba W, Zipes DP. Risk Stratification for Arrhythmic Sudden Cardiac Death. *Circulation* 2011;**123**:2423–2430.

7. Kim RJ, Fieno DS, Parrish TB, Harris K, Chen E-L, Simonetti O, Bundy J, Finn JP, Klocke FJ, Judd RM. Relationship of MRI Delayed Contrast Enhancement to Irreversible Injury, Infarct Age, and Contractile Function. *Circulation* 1999;**100**:1992–2002.

8. Haghbayan H, Lougheed N, Deva DP, Chan KKW, Lima JAC, Yan AT. Peri-Infarct Quantification by Cardiac Magnetic Resonance to Predict Outcomes in Ischemic Cardiomyopathy. *Circulation: Cardiovascular Imaging* 2019;**12**.

9. Disertori M, Rigoni M, Pace N, Casolo G, Masè M, Gonzini L, Lucci D, Nollo G, Ravelli F. Myocardial Fibrosis Assessment by LGE Is a Powerful Predictor of Ventricular Tachyarrhythmias in Ischemic and Nonischemic LV Dysfunction. *JACC: Cardiovascular Imaging* 2016;**9**:1046–1055.

10. Balaban G, Halliday BP, Porter B, Bai W, Nygård S, Owen R, Hatipoglu S, Ferreira ND, Izgi C, Tayal U, Corden B, Ware J, Pennell DJ, Rueckert D, Plank G, Rinaldi CA, Prasad SK, Bishop MJ. Late-Gadolinium Enhancement Interface Area and Electrophysiological Simulations Predict Arrhythmic Events in Patients With Nonischemic Dilated Cardiomyopathy. *JACC: Clinical Electrophysiology* 2021;**7**:238–249.

11. Arevalo HJ, Vadakkumpadan F, Guallar E, Jebb A, Malamas P, Wu KC, Trayanova NA. Arrhythmia risk stratification of patients after myocardial infarction using personalized heart models. *Nature Communications* Nature Publishing Group; 2016;**7**:11437.

12. Balaban G, Halliday BP, Bai W, Porter B, Malvuccio C, Lamata P, Rinaldi CA, Plank G, Rueckert D, Prasad SK, Bishop MJ. Scar shape analysis and simulated electrical instabilities in a non-ischemic dilated cardiomyopathy patient cohort. McCulloch AD, ed. *PLOS Computational Biology* 2019;**15**:e1007421.

13. Hicks KA, Tcheng JE, Bozkurt B, Chaitman BR, Cutlip DE, Farb A, Fonarow GC, Jacobs JP, Jaff MR, Lichtman JH, Limacher MC, Mahaffey KW, Mehran R, Nissen SE, Smith EE, Targum SL, American College of Cardiology, American Heart Association. 2014 ACC/AHA Key Data Elements and Definitions for Cardiovascular Endpoint Events in Clinical Trials: A Report of the American College of Cardiology/American Heart Association Task Force on Clinical Data Standards (Writing Committee to Develop Cardiovascu. *Circulation* 2015;**132**:302–361.

14. Buxton AE, Calkins H, Callans DJ, DiMarco JP, Fisher JD, Greene HL, Haines DE, Hayes DL, Heidenreich PA, Miller JM, Poppas A, Prystowsky EN, Schoenfeld MH, Zimetbaum PJ, Heidenreich PA, Goff DC, Grover FL, Malenka DJ, Peterson ED, Radford MJ, Redberg RF, American College of Cardiology, American Heart Association Task Force on Clinical Data Standards, (ACC/AHA/HRS Writing Committee to Develop Data Standards on Electrophysiology). ACC/AHA/HRS 2006 key data elements and definitions for electrophysiological studies and procedures: a report of the American College of Cardiology/American Heart Association Task Force on Clinical Data Standards (ACC/AHA/HRS Writing Committee to Develop D. *Journal of the American College of Cardiology* 2006;**48**:2360–2396.

15. Haghbayan H, Lougheed N, Deva DP, Chan KKW, Lima JAC, Yan AT. Peri-Infarct Quantification by Cardiac Magnetic Resonance to Predict Outcomes in Ischemic Cardiomyopathy. *Circulation: Cardiovascular Imaging* 2019;**12**:e009156.

16. Schmidt A, Azevedo CF, Cheng A, Gupta SN, Bluemke DA, Foo TK, Gerstenblith G, Weiss RG, Marbán E, Tomaselli GF, Lima JAC, Wu KC. Infarct Tissue Heterogeneity by Magnetic Resonance Imaging Identifies Enhanced Cardiac Arrhythmia Susceptibility in Patients With Left Ventricular Dysfunction. *Circulation* 2007;**115**:2006–2014.

17. Roes SD, Borleffs CJW, Geest RJ van der, Westenberg JJM, Marsan NA, Kaandorp TAM, Reiber JHC, Zeppenfeld K, Lamb HJ, Roos A de, Schalij MJ, Bax JJ. Infarct Tissue Heterogeneity Assessed With Contrast-Enhanced MRI Predicts Spontaneous Ventricular Arrhythmia in Patients With Ischemic Cardiomyopathy and Implantable Cardioverter-Defibrillator. *Circulation: Cardiovascular Imaging* 2009;**2**:183–190.

18. Zegard A, Okafor O, Bono J de, Kalla M, Lencioni M, Marshall H, Hudsmith L, Qiu T, Steeds R, Stegemann B, Leyva F. Myocardial Fibrosis as a Predictor of Sudden Death in Patients With Coronary Artery Disease. *Journal of the American College of Cardiology* 2021;**77**:29–41.

19. Moss AJ, Zareba W, Hall WJ, Klein H, Wilber DJ, Cannom DS, Daubert JP, Higgins SL, Brown MW, Andrews ML. Prophylactic Implantation of a Defibrillator in Patients with Myocardial Infarction and Reduced Ejection Fraction. *New England Journal of Medicine* 2002;**346**:877–883.

20. Bardy GH, Lee KL, Mark DB, Poole JE, Packer DL, Boineau R, Domanski M, Troutman C, Anderson J, Johnson G, McNulty SE, Clapp-Channing N, Davidson-Ray LD, Fraulo ES, Fishbein DP, Luceri RM, Ip JH. Amiodarone or an Implantable Cardioverter–Defibrillator for Congestive Heart Failure. *New England Journal of Medicine* 2005;**352**:225–237.

21. Dagres N, Hindricks G. Risk stratification after myocardial infarction: is left ventricular ejection fraction enough to prevent sudden cardiac death? *European heart journal* 2013;**34**:1964–1971.

22. Wellens HJJ, Schwartz PJ, Lindemans FW, Buxton AE, Goldberger JJ, Hohnloser SH, Huikuri H v., Kaab S, Rovere MT la, Malik M, Myerburg RJ, Simoons ML, Swedberg K, Tijssen J, Voors AA, Wilde AA. Risk stratification for sudden cardiac death: current status and challenges for the future. *European Heart Journal* 2014;**35**:1642–1651.

23. Piers SRD, Tao Q, Riva Silva M de, Siebelink H-M, Schalij MJ, Geest RJ van der, Zeppenfeld K. CMR–Based Identification of Critical Isthmus Sites of Ischemic and Nonischemic Ventricular Tachycardia. *JACC: Cardiovascular Imaging* 2014;**7**:774–784.

24. Wijnmaalen AP, Geest RJ van der, Huls van Taxis CFB van, Siebelink H-MJ, Kroft LJM, Bax JJ, Reiber JHC, Schalij MJ, Zeppenfeld K. Head-to-head comparison of contrast-enhanced magnetic resonance imaging and electroanatomical voltage mapping to assess post-infarct scar characteristics in patients with ventricular tachycardias: real-time image integration and reversed registration. *European Heart Journal* 2011;**32**:104–114.

25. Gould J, Porter B, Claridge S, Chen Z, Sieniewicz BJ, Sidhu BS, Niederer S, Bishop MJ, Murgatroyd F, Ganeshan B, Carr-White G, Razavi R, Chiribiri A, Rinaldi CA. Mean entropy

predicts implantable cardioverter-defibrillator therapy using cardiac magnetic resonance texture analysis of scar heterogeneity. *Heart Rhythm* 2019;**16**:1242–1250.

26. Androulakis AFA, Zeppenfeld K, Paiman EHM, Piers SRD, Wijnmaalen AP, Siebelink H-MJ, Sramko M, Lamb HJ, Geest RJ van der, Riva M de, Tao Q. Entropy as a Novel Measure of Myocardial Tissue Heterogeneity for Prediction of Ventricular Arrhythmias and Mortality in Post-Infarct Patients. *JACC: Clinical Electrophysiology* 2019;**5**:480–489.

27. Kotu LP, Engan K, Borhani R, Katsaggelos AK, Ørn S, Woie L, Eftestøl T. Cardiac magnetic resonance image-based classification of the risk of arrhythmias in post-myocardial infarction patients. *Artificial Intelligence in Medicine* Elsevier B.V.; 2015;**64**:205–215.

28. Sánchez-Somonte P, Quinto L, Garre P, Zaraket F, Alarcón F, Borràs R, Caixal G, Vázquez S, Prat S, Ortiz-Perez JT, Perea RJ, Guasch E, Tolosana JM, Berruezo A, Arbelo E, Sitges M, Mont L, Roca-Luque I. Scar channels in cardiac magnetic resonance to predict appropriate therapies in primary prevention. *Heart Rhythm* 2021;**18**:1336–1343.

29. Flett AS, Hasleton J, Cook C, Hausenloy D, Quarta G, Ariti C, Muthurangu V, Moon JC. Evaluation of Techniques for the Quantification of Myocardial Scar of Differing Etiology Using Cardiac Magnetic Resonance. *JACC: Cardiovascular Imaging* 2011;**4**:150–156.

30. Wu KC. Sudden Cardiac Death Substrate Imaged by Magnetic Resonance Imaging. *Circulation: Cardiovascular Imaging* 2017;**10**:1–29.

Tables

Table 1: Scar microstructure features.

Scar feature	Feature description
Transmurality	The extent of spread of LGE emanating outwards from the endocardium to epicardium, calculated using a ray tracing method.
Radiality	Quantification of the angular variance of LGE in relation to the centre of the LV blood pool.
PIZ islets	Regions of PIZ contained within core scar or an area of PIZ encapsulated by core scar and either endocardial or epicardial boundaries.
Number of components	The degree of connectivity between LGE across the LV.
Interface area	The extent of the border between myocardium and LGE.
Entropy	The level of disorder within the LGE. Calculated by applying standard Shannon entropy[26]
Gradient	The rate of change in LGE intensity.

The 7 groups of morphological (top 5 rows) and texture (bottom 2 rows) related scar features that were extracted from the LGE images.
LGE = late gadolinium enhancement; LV = left ventricle; PIZ = peri-infarct zone

Table 2: Baseline characteristics.

Variable	N (%)/mean (SD)/median (IQR)	PIZ<8.76g	PIZ≥8.76g	P-value
Demographics				
Age (years)	64.4 (9.9)	65.2 (9.5)	63.6 (10.2)	0.10
Female	61 (14.0)	41 (18.8)	20 (9.1)	0.004
Caucasian	357 (81.7)	178 (81.7)	179 (81.7)	0.98
BMI (kg/m2)	27.8 (5.0)	27.6 (4.7)	28.0 (5.2)	0.34
Heart rate (bpm)	69.3 (13.3)	69.4 (14.1)	69.3 (12.6)	0.92
SBP (mmHg)	126.5 (19.3)	130.8 (19.4)	122.5 (18.3)	<0.001
DBP (mmHg)	73.3 (11.7)	75.3 (11.5)	71.4 (11.7)	<0.001
Significant CAD*	412 (95.4)	198 (91.2)	214 (99.5)	<0.001
CAD type				0.15
Single vessel	131 (31.8)	72 (36.4)	59 (27.6)	
2 vessels	117 (28.4)	51 (25.8)	66 (30.8)	
3 vessels	164 (39.8)	75 (37.9)	89 (41.6)	
Prior MI	316 (72.3)	141 (64.7)	175 (79.9)	<0.001
History of PCI	225 (51.5)	119 (54.6)	106 (48.4)	0.20
History of CABG	121 (27.7)	58 (26.6)	63 (28.8)	0.61
Hypertension	231 (52.9)	116 (53.2)	115 (52.5)	0.88
Diabetes mellitus	128 (29.3)	59 (27.1)	69 (31.5)	0.31
Documented hypercholesterolemia	356 (81.5)	171 (78.4)	185 (84.5)	0.10
Documented family history of premature CAD	95 (21.7)	50 (22.9)	45 (20.5)	0.54

Smoking status				0.01
Yes	45 (10.3)	19 (8.8)	26 (11.9)	
Ex-smoker	242 (55.5)	109 (50.2)	133 (60.7)	
No	149 (34.2)	89 (41.0)	60 (27.4)	
Baseline AF	73 (16.7)	33 (15.1)	40 (18.3)	0.38
NYHA functional class				0.17
I	145 (33.3)	81 (37.3)	64 (29.4)	
II	197 (45.3)	95 (43.8)	102 (46.8)	
III or IV	93 (21.4)	41 (18.9)	52 (23.9)	
Medications				
Antithrombotic therapy	420 (96.1)	210 (96.3)	210 (95.9)	0.81
Diuretic	204 (46.7)	72 (33.0)	132 (60.3)	<0.001
Beta-blocker	338 (77.3)	158 (72.5)	180 (82.2)	0.02
ACEi/ARB	368 (84.2)	168 (77.1)	200 (91.3)	<0.001
Lipid-lowering drug	386 (88.3)	188 (86.2)	198 (90.4)	0.17
Aldosterone antagonist	108 (24.7)	31 (14.2)	77 (35.2)	<0.001
CMR volumetric measurements				
LVEF (%)	47.2 (16.8)	55.2 (16.0)	39.2 (13.3)	<0.001
LV mass indexed (g/m2)	79.1 (24.6)	72.1 (20.9)	86.0 (26.0)	<0.001
LVEDVi (ml/m2)	106.5 (40.8)	89.1 (28.9)	123.7 (43.5)	<0.001
RVEF (%)	58.1 (12.7)	59.4 (11.2)	56.8 (13.9)	0.03

RVEDVi (ml/m2), median (IQR)	73.1 (62.2-85.6)	73.3 (64.0-83.8)	73.0 (61.0-86.9)	0.76
CMR LGE characteristics				
Infarct pattern LGE	378 (86.5)	159 (72.9)	219 (100.0)	<0.001
Predominant territory				0.010
Anterior	172 (45.5)	60 (37.7)	112 (51.1)	
Lateral	54 (14.3)	31 (19.5)	23 (10.5)	
Inferior	152 (40.2)	68 (42.8)	84 (38.4)	
Multi-territory infarct	120 (31.7)	22 (13.8)	98 (44.7)	<0.001
No. infarcted segments, median (IQR)	5.0 (2.0-7.0)	3.0 (0.0-5.0)	7.0 (5.0-9.0)	<0.001
PIZ mass (g), median (IQR)	8.8 (4.2-14.4)	NA	NA	NA
Infarct core mass (g), median (IQR)	17.6 (6.5-30.2)	6.4 (0.0-12.8)	29.0 (20.8-39.6)	<0.001

ACEi = angiotensin-converting enzyme inhibitor; AF = atrial fibrillation; ARB = angiotensin II receptor blocker; BMI = body mass index; CABG = coronary artery bypass graft CAD = coronary artery disease; CMR = cardiovascular magnetic resonance; DBP = diastolic blood pressure; ECG = electrocardiogram; IQR = interquartile range; LVEDVi = indexed left ventricular end-diastolic volume; LVEF = Left ventricular ejection fraction; MI = myocardial infarction; NA = not applicable; NYHA = New York Heart Association; RVEDVi = indexed right ventricular end-systolic volume; PIZ = peri-infarct zone; PCI = percutaneous coronary intervention; SBP = systolic blood pressure. *includes patients with prior coronary revascularisation.

Table 3: Performance of scar microstructure features

Scar feature	Scar feature description	Model C-statistic	Scar feature HR and 95% CI	Scar feature P-value
sum core entropy	Sum of core infarct entropy score from all LGE slices	0.74	1.68 (1.27 - 2.21)	<0.001
sum core SD transmurality	Sum of core infarct transmurality SD from all LGE images	0.73	2.03 (1.44 - 2.86)	<0.001
sum PIZ entropy	Sum of the PIZ entropy score from all LGE slices	0.73	2.03 (1.43 - 2.88)	0.001
sum core transmurality	Sum of core infarct transmurality from all LGE slices	0.723	1.65 (1.22 - 2.23)	<0.001
sum core & PIZ combined entropy	Sum of the combined entropy score from core infarct and the PIZ from all LGE slices	0.72	2.23 (1.52 - 3.27)	<0.001
sum core transmurality LC	sum of the core infarct transmurality of the LC from all LGE slices	0.71	1.65 (1.23 - 2.21)	<0.001
core interface area	Border zone area of the core infarct and adjacent tissue	0.70	1.62 (1.23 - 2.12)	0.001
mean core transmurality LC	Mean transmurality of core infarct in the LC across all LGE slices	0.69	1.74 (1.24 - 2.44)	0.004
sum PIZ components	Sum of the number of PIZ components from all LGE slices	0.69	1.32 (1.03 - 1.7)	0.01
core & PIZ combined interface area LC	Combined border zone area of the core infarct and PIZ in the LC	0.69	1.52 (1.17 - 1.96)	0.001
mean core SD transmurality	Mean SD of the core infarct transmurality across all LGE slices	0.69	1.75 (1.23 - 2.5)	0.001
core & PIZ combined interface area	Combined border zone area of the core infarct and PIZ	0.69	1.44 (1.11 - 1.86)	0.006
sum core radiality	Sum core infarct radiality across from LGE slices	0.69	1.53 (1.14 - 2.06)	0.006
PIZ interface area	Border zone area between the PIZ and adjacent tissue	0.68	1.56 (1.19 - 2.05)	<0.001
PIZ interface area LC	Border zone area of the PIZ and adjacent tissue in the LC	0.68	1.45 (1.12 - 1.89)	0.004

mean PIZ entropy	Mean entropy score of the PIZ across all LGE slices	0.68	1.87 (1.26 - 2.75)	0.003
core interface area LC	Border zone area between core infarct and adjacent tissue in the LC	0.68	1.63 (1.26 - 2.1)	<0.001
sum PIZ gradient	Sum of the PIZ gradient from all LGE slices	0.68	1.62 (1.2 - 2.21)	0.011
sum core components	Sum of the number of core infarct components from all LGE slices	0.68	1.38 (1.07 - 1.78)	0.016
mean core entropy	Mean entropy score of the core infarct across all LGE slices	0.68	1.93 (1.29 - 2.88)	<0.001
mean core transmurality	Mean core infarct transmurality across all LGE slices	0.67	1.64 (1.19 - 2.28)	0.005
mean core & PIZ combined entropy	Combined mean entropy score of the core infarct and PIZ across all LGE slices	0.67	1.91 (1.26 - 2.9)	0.001
mean core radiality	Mean core infarct radiality across all LGE slices	0.66	1.33 (1.0 - 1.78)	0.005
SD core transmurality	SD of the core infarct transmurality	0.66	1.36 (0.96 - 1.93)	0.03
sum core radiality LC	Sum core infarct radiality from all LGE slices	0.66	1.33 (1.04 - 1.71)	0.02
sum core & PIZ combined components	Sum of the number of core infarct and PIZ components from all LGE slices	0.65	1.22 (0.96 - 1.56)	0.009
mean core radiality LC	Mean core infarct radiality in the LC across all LGE slices	0.65	1.31 (1.04 - 1.65)	0.046
mean PIZ gradient	Mean PIZ gradient across all LGE slices	0.64	1.46 (1.06 - 2.01)	0.043

Performance of all scar features significantly associated with the primary endpoint after adjustment LVEF <35% and NYHA >1. LC = largest component; LGE = late gadolinium enhancement; ICD = implantable cardioverter defibrillator; SD = standard deviation; PIZ = peri-infarct zone

Figures

Figure 1: Kaplan-Meier plots of the primary endpoint by tertiles of LGE metric.

Top row: Kaplan-Meier plots of the primary endpoint by tertiles of peri-infarct zone mass. Bottom row: Kaplan-Meier plots of the primary endpoint by tertiles of core infarct mass. ASCD = aborted SCD; SCD = sudden cardiac death.

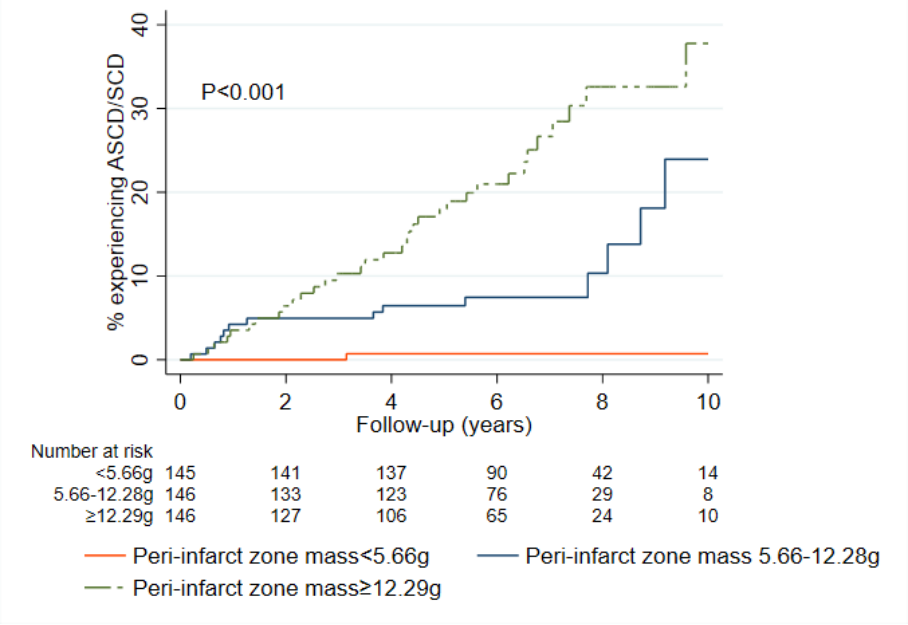

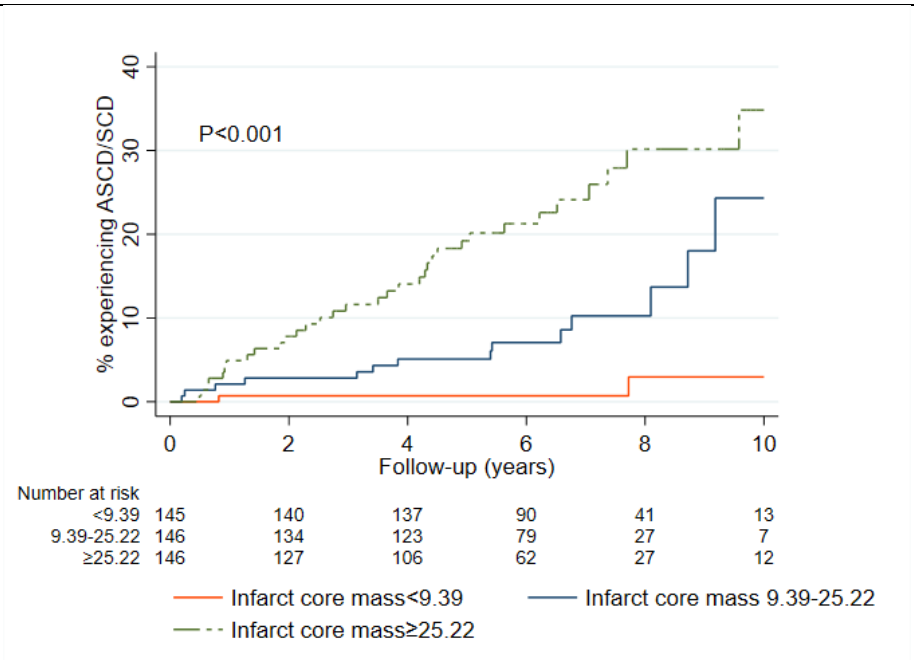

Figure 2: Multivariable Model 1 for the primary endpoint with subsequent addition of LGE metrics.

Top row: To mirror current clinical guidelines for ICD implantation, a multivariable model using binary cut-offs of LVEF <35% and NYHA class >1 was generated with subsequent addition of the LGE quantification data.
Bottom row: Forest plot of the final multivariable model presented using LGE results per 10grams.
CI = confidence interval; HR = hazard ratio; LVEF = Left ventricular ejection fraction; PIZ = peri-infarct zone.

Variable	HR (95% CI)	P-value
LVEF<35%	3.09 (1.75, 5.45)	<0.001
NYHA 2, 3 or 4	1.33 (0.70, 2.52)	0.39
Harrell's C-statistic = 0.64		

Variable	HR (95% CI)	P-value
PIZ mass (per g)	1.07 (1.02, 1.12)	0.002
PIZ mass (per 10g)	1.95 (1.28, 2.98)	
Infarct core mass (per g)	1.03 (1.01, 1.05)	0.01
Infarct core mass (per 10g)	1.28 (1.06, 1.56)	
LVEF<35%	1.65 (0.90, 3.03)	0.11
NYHA 2, 3 or 4	1.20 (0.63, 2.30)	0.58
Harrell's C-statistic = 0.79		

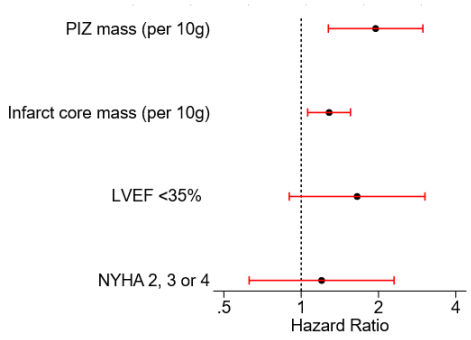

Figure 3: Competing risk analysis.

Competing risk survival analysis for the primary endpoint; SCD/aborted SCD versus other cause of death. CI = confidence interval; sHR = subdistribution hazard ratio; LVEF = left ventricular ejection fraction; NYHA = New York Heart Association; PIZ = peri-infarct zone.

Variable	sHR (95% CI)	P-value
LVEF<35%	2.66 (1.51, 4.69)	0.001
NYHA 2, 3 or 4	1.20 (0.64, 2.27)	0.57

Variable	sHR (95% CI)	P-value
PIZ mass (g)	1.07 (1.03, 1.12)	0.001
Infarct core mass (g)	1.03 (1.01, 1.04)	0.003
LVEF<35%	1.42 (0.80, 2.53)	0.23
NYHA 2, 3 or 4	1.09 (0.56, 2.11)	0.80

Figure 4: Multivariable Model 2 for the primary endpoint with subsequent addition of LGE metrics.

Top row: To select this model, a forward stepwise procedure was applied with p<0.10 as the criterion for inclusion, forcing in recognised predictors of the outcome (age, sex and LVEF) with simultaneous addition of LGE quantification data.
Bottom row: Forest plot of the final multivariable model presented using LGE results per 10grams.

Variable	HR (95% CI)	P-value
Age (per 10 years)	0.76 (0.57, 1.02)	0.07
Female	0.31 (0.07, 1.28)	0.11
LVEF (%)	0.96 (0.95, 0.98)	<0.001
ACE-i/ARB	6.32 (0.87, 46.15)	0.07
Smoking status		0.04
Non-smoker	Reference group	
Ex-smoker	1.57 (0.77, 3.17)	
Current smoker	2.61 (1.05, 6.44)	
Atrial fibrillation	1.98 (1.01, 3.90)	0.05
Harrell's C-statistic = 0.76		

Variable	HR (95% CI)	P-value
PIZ mass (per g)	1.07 (1.02, 1.12)	0.005
PIZ mass (per 10 g)	1.93 (1.22, 3.06)	
Infarct core mass (per g)	1.02 (1.00, 1.05)	0.03
Infarct core mass (per 10g)	1.27 (1.03, 1.58)	
Age (per 10 years)	0.96 (0.71, 1.29)	0.78
Female	0.33 (0.08, 1.39)	0.13
LVEF (%)	0.99 (0.97, 1.02)	0.63
ACE-i/ARB	4.70 (0.64, 34.57)	0.13
Smoking status		0.04
Non-smoker	Reference group	
Ex-smoker	1.30 (0.64, 2.65)	
Current smoker	2.71 (1.08, 6.80)	
Atrial fibrillation	2.37 (1.19, 4.75)	0.02
Harrell's C-statistic = 0.82		

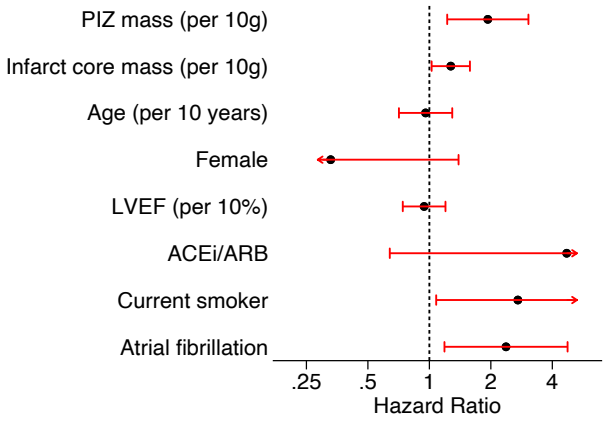

Figure 5: Significant scar feature groups on computational analysis

Example LGE-CMR images demonstrating the 6 groups containing features that were significantly associated with the primary outcome on multivariable analysis. Top row: High feature value. Bottom row: Low feature value. Core scar demonstrated in red and the PIZ in pink in images 1-4. 1. Interface area, a measure of the boundary length between LGE and adjacent tissue (yellow line); 2. Scar transmurality, a measure describing the extent of spread of LGE from the endocardium to epicardium; 3. Scar radiality, a measure of the circumferential radiation of the LGE taken from the centre of the left ventricular blood pool; 4. No. components, the amount of connectivity between LGE across the LV; 5. Entropy, a measure of the disorder within the LGE. Calculated by applying standard Shannon entropy; 6. Gradient, the rate of change in LGE intensity.
CMR = cardiovascular magnetic resonance; LGE = late gadolinium enhancement; PIZ = peri-infarct zone.

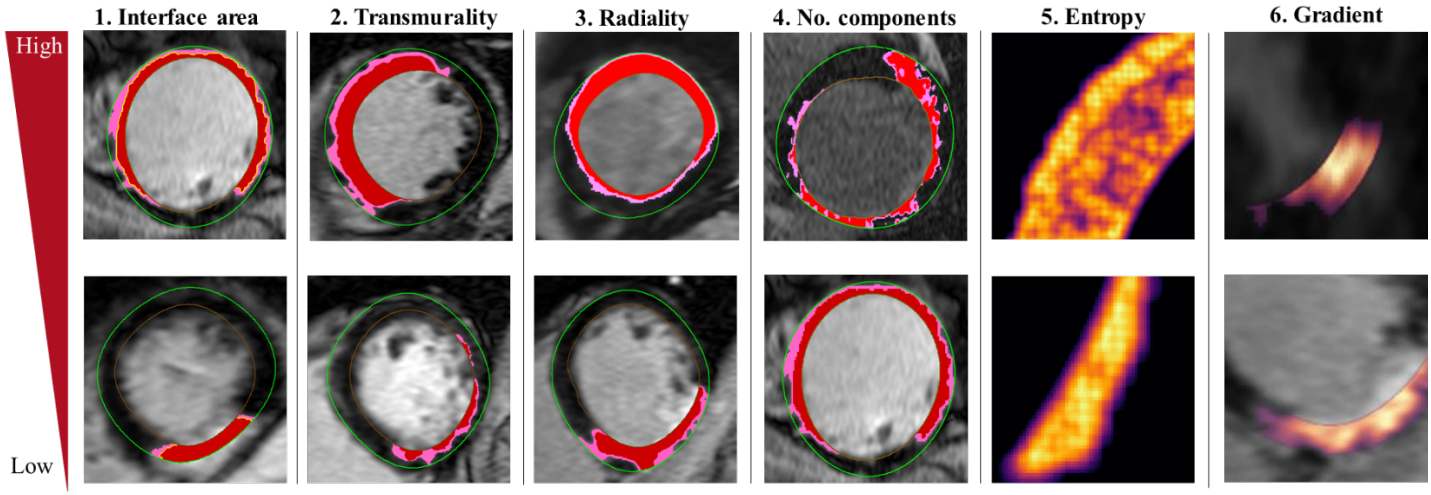

Figure 6: Multivariable analysis of specific scar microstructure features.

Best performing scar microstructure models within each group, each model adjusted for LVEF <35% and NYHA Class II, III, or IV. PIZ = peri-infarct zone.

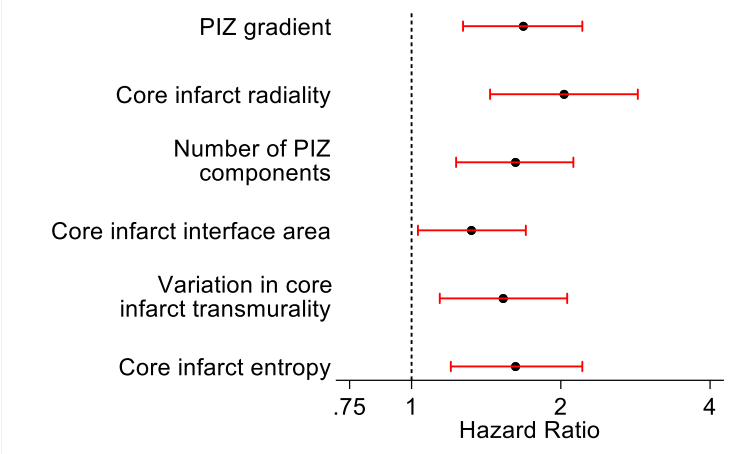

Figure 7: Multivariable Model 2 for major heart events with subsequent addition of LGE metrics

Top row: Multivariable model for the primary endpoint using a forward stepwise procedure, applying p<0.10 as the criterion for inclusion, forcing in recognised predictors of the outcome (age, sex and LVEF).
Bottom row: Forest plot of the final multivariable model presented using LGE results per 10grams.
BMI = body mass index; CI = confidence interval; HR = hazard ratio; LVEF = Left ventricular ejection fraction; PIZ = peri-infarct zone

Variable	HR (95% CI)	P-value
Age (per 10 years)	1.42 (1.07, 1.87)	0.01
Female	1.35 (0.70, 2.61)	0.37
LVEF (%)	0.95 (0.93, 0.96)	<0.001
Diabetes	1.93 (1.20, 3.11)	0.007
Atrial fibrillation	1.98 (1.20, 3.25)	0.007
BMI (kg/m^2)	1.06 (1.01, 1.11)	0.01
Prior revascularisation	1.94 (1.14, 3.30)	0.02
Harrell's C-statistic = 0.79		

Variable	HR (95% CI)	P-value
PIZ mass (per g)	1.02 (0.98, 1.06)	0.35
PIZ mass (per 10g)	1.22 (0.81, 1.82)	
Infarct core mass (per g)	1.00 (0.98, 1.02)	0.77
Infarct core mass (per 10g)	1.03 (0.85, 1.25)	
Age (per 10 years)	1.49 (1.12, 1.97)	0.006
Female	1.37 (0.71, 2.64)	0.35
LVEF (%)	0.95 (0.93, 0.97)	<0.001
Diabetes	1.93 (1.20, 3.11)	0.007
Atrial fibrillation	2.04 (1.23, 3.38)	0.006
BMI (kg/m^2)	1.05 (1.01, 1.10)	0.02
Prior revascularisation	1.87 (1.10, 3.18)	0.02
Harrell's C-statistic = 0.79		

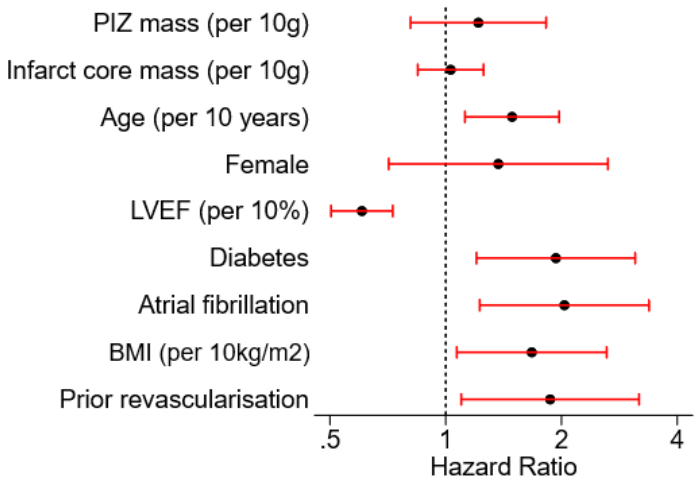

Figure 8: Multivariable Model 2 for all-cause mortality with subsequent addition of LGE metrics

Top row: Multivariable model for all-cause mortality using a forward stepwise procedure, applying p<0.10 as the criterion for inclusion, forcing in recognised predictors of the outcome (age, sex and LVEF).
Bottom row: Forest plot of the final multivariable model presented using LGE results per 10grams.
CI = confidence interval; HR = hazard ratio; LVEF = Left ventricular ejection fraction; PIZ = peri-infarct zone.

Variable	HR (95% CI)	P-value
Age (per 10 years)	1.64 (1.34, 2.00)	<0.001
Female	0.93 (0.56, 1.56)	0.79
LVEF (%)	0.97 (0.96, 0.98)	<0.001
Diabetes	1.87 (1.32, 2.64)	<0.001
Atrial fibrillation	1.53 (1.04, 2.24)	0.03
Harrell's C-statistic = 0.74		

Variable	HR (95% CI)	P-value
PIZ mass (per g)	1.04 (1.01, 1.08)	0.02
PIZ mass (per 10g)	1.50 (1.08, 2.09)	
Infarct core mass (per g)	1.00 (0.98, 1.02)	0.96
Infarct core mass (per 10g)	1.00 (0.84,1.18)	
Age (per 10 years)	1.79 (1.45, 2.20)	<0.001
Female	0.99 (0.59, 1.66)	0.98
LVEF (%)	0.98 (0.96, 0.99)	<0.001
Diabetes	1.86 (1.32, 2.64)	<0.001
Atrial fibrillation	1.55 (1.05, 2.28)	0.03
Harrell's C-statistic = 0.75		

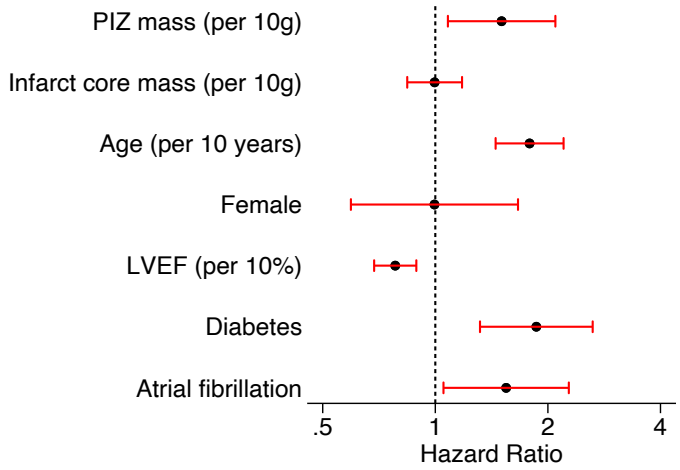

Figure 9:

Multivariable models for the primary endpoint in patients with LVEF ≥35% with subsequent addition of LGE metrics
CI = confidence interval; HR = hazard ratio; LVEF = Left ventricular ejection fraction; PIZ = peri-infarct zone.

Variable	HR (95% CI)	P-value
Age (per 10 years)	0.89 (0.59, 1.33)	0.57
Female	0.25 (0.03, 1.83)	0.17
LVEF (%)	0.95 (0.91, 0.98)	0.003
Harrell's C-statistic = 0.69		

Variable	HR (95% CI)	P-value
PIZ mass (g)	1.02 (0.94, 1.11)	0.58
Infarct core mass (g)	1.03 (0.99, 1.07)	0.13
Age (per 10 years)	1.07 (0.70, 1.65)	0.76
Female	0.26 (0.03, 1.90)	0.18
LVEF (%)	0.98 (0.93, 1.03)	0.38
Harrell's C-statistic = 0.76		